$(c\text{-}C_3D_4)^{\bullet-}$ (11%). Only the two adducts $(OC)_3Mn(D)(c\text{-}C_3D_5)^-$ (≈20%) and $(OC)_3Mn(D)_2(c\text{-}C_3D_4)^-$ (≈80%) were formed in the reaction with $(OC)_3Mn^-$.

The small kinetic isotope effects observed for the $(OC)_2Fe^{\bullet-}$ (1.2 ± 0.1) and $(OC)_3Mn^-$ reactions (1.9 ± 0.3) suggest the intervention of secondary isotope effects that *increase* the rate constants of the cyclopropane-d_6 reactions. The secondary effects are the increase in the density of states and lifetimes of the excited deuterated adducts that result in an increase in the collisional quenching efficiency of these species. The larger quenching efficiency not only influences the yields of the intermediates involved in the product channel, but reduces the extent of the reductive elimination of cyclopropane-d_6 from **7***-d_6 (k_{-1}). It is this latter factor that inflates k_{total} for the cyclopropane-d_6 reactions and masks the isotope effect for the oxidative insertion step. This is most clearly seen in the results of the $(OC)_2Fe^{\bullet-}$ reaction with cyclopropane-d_6, where the major product ions are those formed in the initial intermolecular step. The larger isotope effect observed for the $(OC)_3Mn^-$ reactions arises because the major product adduct ions result from the additional step of an intramolecular deuterium shift (k_2) and its attendant normal isotope effect.

The present results are consistent with the available data on the reactions of $(OC)_2Fe^{\bullet-}$ and $(OC)_3Mn^-$ with alkanes and other cycloalkanes,[17] and establish the intermediacy of the related **7*** and **8*** ions in the mechanism of dehydrogenation of these substrates.

Acknowledgment. The authors are pleased to acknowledge the financial support of the National Science Foundation for this research.

Registry No. 1, 137007-86-4; **1**-d_6, 137007-88-6; **2**, 137007-87-5; **2**-d_4, 137007-89-7; **4**, 137007-90-0; **4**-d_6, 137007-92-2; **6**, 137007-91-1; $(C\text{-}O)_3Mn^-$, 101953-17-7; $(CO)_2Fe^{\bullet-}$, 71701-39-8; $c\text{-}C_3H_6$, 75-19-4; $c\text{-}C_3D_6$, 2207-64-9.

Application of the Xenon-Adsorption Method for the Study of Metal Cluster Formation and Growth on Y Zeolite

Ryong Ryoo,* Sung June Cho, Chanho Pak, Jeong-Guk Kim,† Son-Ki Ihm,† and Jeong Yong Lee‡

Department of Chemistry and Center for Molecular Science, Department of Chemical Engineering, and Department of Materials Science and Engineering, Korea Advanced Institute of Science and Technology, Taeduk Science Town, Taejon, 305-701 Korea.
Received March 12, 1991

Abstract: Supported metal clusters of Pt, Ir, Ru, Rh, and Pd have been prepared in the supercage of Y zeolite by activating their ion-exchanged ammine complexes. Xenon adsorption isotherms obtained from these samples at temperatures ranging from 296 to 340 K and pressures up to 500 Torr, as well as the chemical shift data from the ^{129}Xe NMR study of the adsorbed xenon gas, indicate that the xenon adsorption can occur quite strongly, becoming saturated above ca. 50 Torr, on the metal cluster surface whereas the adsorption is so weak on the support that the adsorbed quantity increases linearly with pressure according to Henry's law. Upon chemisorption of hydrogen or oxygen, the metal clusters lose the ability to adsorb the xenon so strongly, resulting in a decrease in the xenon adsorption quantity. Such a xenon-adsorption decrease due to the chemisorption of another gas can determine the amount of xenon that can be saturated on all the metal clusters present in the sample. This quantity is sensitive to the size and the number of the supported clusters. It can then be used to probe the formation and the size variation of the clusters which are very difficult to study by other methods due to their very small size, e.g. about 1 nm. An application of such a simple technique for the study of Pt cluster formation on NaY zeolite indicates that the size of the Pt cluster formed in the supercage does not change significantly as the metal content is changed from 2 to 10%. This xenon-adsorption method has also been very useful for the study of the formation and growth of the Ru cluster on NaY zeolite. The result indicates that very small Ru clusters are formed in the supercage by treating a precursor, which is prepared by heating NaY zeolite in an aqueous ammonia solution of $RuCl_3$, in vacuum at temperatures above 623 K. The clusters grow gradually at higher temperatures both in H_2 and under vacuum. The data also agree that an exposure of the supported Ru clusters in O_2 at temperatures above 423 K causes excessive migration of the Ru species, resulting in large agglomeration. Another example, which can further promise wide applicability of the xenon adsorption method, is a study of the formation of Pd clusters in the supercage of various ion-exchanged Y and X zeolites. The result indicates that Ca^{2+}, Y^{3+}, and perhaps other multivalent cations residing in the supercage are necessary to obtain ca. 1-nm clusters whereas univalent cations give larger clusters.

Introduction

Metal clusters supported on Y zeolite, of ca. 1 nm, can be a suitable subject for the adsorption and catalysis of very small clusters.[1] The effect of the cluster-size variation on the chemisorptive and catalytic properties of the small metal cluster is particularly interesting since its understanding may build a bridge between homogeneous catalysis and heterogeneous catalysis. However, such a study requires a very precise method to determine the cluster size to the level of the number of atoms per cluster. A few approaches for the determination of the average number of metal atoms per cluster supported on Y zeolites using certain assumptions have been reported,[2,3] but in general their results failed to agree with those obtained by other methods such as transmission electron microscopy (TEM),[4-6] extended X-ray absorption fine

* Author to whom correspondence should be addressed at the Department of Chemistry.
† Department of Chemical Engineering.
‡ Department of Materials Science and Engineering.

(1) Jacobs, P. A. In *Metal Clusters in Catalysis*; Gates, B. C., Guczi, L., Knozinger, H., Eds.; Elsevier: Amsterdam, 1986; p 357.
(2) Dalla Betta, R. A.; Boudart, M. In *Proceedings of the 5th International Congress on Catalysis, Palm Beach*; Hightower, J., Ed.; North Holland: Amsterdam, 1973; Vol. 2, p 1329.
(3) de Menorval, L.-C.; Fraissard, J. P.; Ito, T. *J. Chem. Soc., Faraday Trans. 1* **1982**, *78*, 403.
(4) Gallezot, P.; Mutin, I.; Dalmai-Imelik, G.; Imelik, B. *J. Microsc. Spectrosc. Electron* **1976**, *1*, 1.

0002-7863/92/1514-76$03.00/0

Table I. Unit Cell Formulas for Various Zeolite Samples

sample	unit cell formula
NaY	$Na_{56}[(AlO_2)_{56}(SiO_2)_{136}]$
NaX	$Na_{80}[(AlO_2)_{80}(SiO_2)_{112}]$
CaY	$Na_{18}Ca_{19}[(AlO_2)_{56}(SiO_2)_{136}]$
YY	$Na_{14}Y_{14}[(AlO_2)_{56}(SiO_2)_{136}]$
YX	$Na_{20}Y_{20}[(AlO_2)_{80}(SiO_2)_{112}]$
KY	$K_{56}[(AlO_2)_{56}(SiO_2)_{136}]$

structure (EXAFS),[5] wide-angle X-ray scattering (WAXS),[5,7,8] and small-angle X-ray scattering (SAXS).[9]

One of the most fascinating modern techniques developed for the study of the zeolite-supported metal clusters is the use of ^{129}Xe NMR spectroscopy of the adsorbed xenon gas.[3,10-14] This ^{129}Xe NMR method is based on the fact that the line shape and the chemical shift are very sensitive to the metal species present in the zeolite cages or channels. Previous studies using the ^{129}Xe NMR spectroscopic method reported that the zeolite-supported metal sample gave much greater chemical shifts than the zeolite support under the same experimental conditions. However, the chemical shift difference between the supported sample and the zeolite support decreased as the xenon pressure was increased. Similar results were reported when divalent cations were exchanged into the NaY zeolite.[15-18] Such a chemical shift variation observed for the exchange of divalent cations was first attributed to an electric field effect arising from the cation.[15,16] Recently, the chemical shift variation was explained by a rapid xenon exchange between strong adsorption sites.[17] The rate of xenon exchange depends on the temperature and the size of zeolite crystals.[14,19] Very fast exchange of xenon averages the chemical shift of xenon over many of the adjacent 1-μm zeolite microcrystals at room temperature. At 173 K, the xenon exchange occurs much more slowly, but it is still fast enough to average completely the chemical shift of xenon between the supported metal cluster and the zeolite support. It may be expected that the chemical shift dependence of zeolite-supported metal samples is also due to a strong adsorption of xenon on the metal cluster. The present study indeed clarifies that the xenon can be adsorbed quite strongly on the metal cluster, compared with the zeolite support, and therefore the xenon adsorption becomes nearly saturated on the metal cluster at considerably low pressures, e.g. 50 Torr at 296 K, while the adsorption on the zeolite surface increases linearly with pressure according to Henry's law.

The total amount of xenon which can be saturated on the metal clusters in a given sample may be obtained by analyzing the xenon adsorption isotherm in a manner similar to the determination of the hydrogen chemisorption on supported platinum catalysts, e.g., by extrapolating the isotherm to zero pressure.[20] Such a determination of the xenon adsorption can give a total surface area summed over all the metal clusters accessible for xenon in the sample, which is shown in this study to be very sensitive to the cluster-size variation. It will then be very interesting and useful to probe the formation and growth of metal clusters by the xenon-adsorption isotherms obtained after various treatments of the zeolite-supported metal samples. Application of such a simple xenon-adsorption technique to the study of Pt, Ru, and Pd clusters is introduced in this paper.

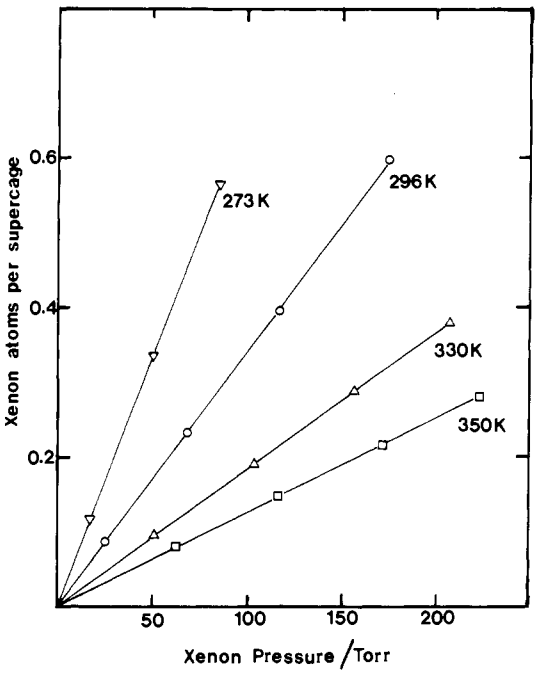

Figure 1. Xenon adsorption plotted against pressure. Xenon-adsorption isotherms from a high-purity NaY zeolite are almost proportional to the pressure since the adsorption is very weak.

Experimental Section

A high-purity NaY sample and a NaX zeolite sample were prepared with high-purity starting materials by the Breck procedures.[21] The zeolites were transformed into K^+, Ca^{2+}, or Y^{3+} ion-exchanged forms by suitable ion-exchange procedures.[21] The unit cell formula of the zeolite, obtained by elemental analysis, is given in Table I.

$Pt(NH_3)_4^{2+}$ was ion exchanged into the NaY zeolite with stirring in an aqueous solution of $[Pt(NH_3)_4]Cl_2$ overnight at room temperature. The zeolite sample was filtered, washed with doubly distilled water, and dried in a vacuum oven at 330 K. This sample was activated by heating linearly to 583 K over 12 h and maintaining at this temperature for 2 h in flowing O_2 (>1 L min^{-1} g^{-1}). The O_2 gas was evacuated at room temperature. The sample was then reduced in flowing H_2 (>200 mL min^{-1} g^{-1}) with linear heating to 573 K over 2 h and maintaining at this temperature for 2 h. Desorption of hydrogen from the surface of the Pt cluster, thus generated, was performed for 2 h at 673 K and 1×10^{-5} Torr. All the sample treatments were performed in situ in a Pyrex U-tube flow reactor which was connected to an NMR tube equipped with a homemade vertical ground-glass vacuum stopcock. The NMR tube was sealed off by a flame after the sample was transferred into the tube. Natural xenon gas (Matheson, 99.995%) was adsorbed on the sample for both the adsorption measurement and the ^{129}Xe NMR experiment. The Pt content of this sample was determined from chemical analysis. The samples are designated as Pt_x/NaY where the subscript x denotes the number of the metal atoms per unit cell of zeolite.

$RuCl_3$ was dissolved in an aqueous solution of ammonia overnight at 350 K. The solution initially contained black $Ru(OH)_3$ precipitate which then turned a slightly greenish yellow color. The NaY zeolite sample was then stirred overnight in this solution at constant temperature. The color of the zeolite turned purple after this treatment due to the formation of a ruthenium red complex ion exchanged in zeolite.[22] This sample was filtered, washed, and dried in the same way as for the preparation of Pt sample. Such a precursor of the zeolite-supported Ru cluster was heated under 1×10^{-5} Torr to a given maximum temperature, e.g. 673 K, typically at a heating rate of 1.1 K min^{-1}, and maintained at this tem-

(5) Boudart, M.; Samant, M. G.; Ryoo, R. *Ultramicroscopy* **1986**, *20*, 125 and references therein.
(6) Chmelka, B. F.; de Menorval, L.-C.; Csencsits, R.; Ryoo, R.; Liu, S. B.; Radke, C. J.; Petersen, E. E.; Pines, A. In *Proceedings of European Conference on Structure and Reactivity of Surfaces*; Morterra, C., Zecchina, A., Costa, G., Eds.; Elsevier: Amsterdam, 1989; p 269.
(7) Gallezot, P.; Bienenstock, A. K.; Boudart, M. *Nouv. J. Chim.* **1978**, *2*, 263.
(8) Samant, M. G.; Bergeret, G.; Meitzner, G.; Gallezot, P.; Boudart, M. *J. Phys. Chem.* **1988**, *92*, 4547.
(9) Gallezot, P.; Alarcon-Diaz, A.; Dalmon, J.-A.; Renouprez, A. J.; Imelik, B. *J. Catal.* **1975**, *39*, 334.
(10) Fraissard, J.; Ito, T. *Zeolites* **1988**, *8*, 350 and references therein.
(11) Chmelka, B. F.; Ryoo, R.; Liu, S. B.; de Menorval, L.-C.; Radke, C. J.; Petersen, E. E.; Pines, A. *J. Am. Chem. Soc.* **1988**, *110*, 4465.
(12) Scharpf, E. W.; Crecely, R. W.; Gates, B. C.; Dybowski, C. *J. Phys. Chem.* **1986**, *90*, 9.
(13) Shoemaker, R.; Apple, T. *J. Phys. Chem.* **1987**, *91*, 4024.
(14) Yang, O. B.; Woo, S. I.; Ryoo, R. *J. Catal.* **1990**, *123*, 375.
(15) Ito, T.; Fraissard, J. *J. Chem. Phys.* **1982**, *76*, 5225.
(16) Ito, T.; Fraissard, J. *J. Chem. Soc., Faraday Trans. 1* **1987**, *83*, 451.
(17) Gedeon, A.; Bonardet, J. L.; Ito, T.; Fraissard, J. *J. Phys. Chem.* **1989**, *93*, 2563.
(18) Bansal, N.; Dybowski, C. *J. Phys. Chem.* **1988**, *92*, 2333.
(19) Ryoo, R.; Pak, C.; Chmelka, B. F. *Zeolites* **1990**, *10*, 790.
(20) Benson, J. E.; Boudart, M. *J. Catal.* **1965**, *4*, 704.
(21) Breck, D. *Zeolite Molecular Sieves*; Wiley: New York, 1974.
(22) Pederson, L. A.; Lunsford, J. H. *J. Catal.* **1980**, *61*, 39.

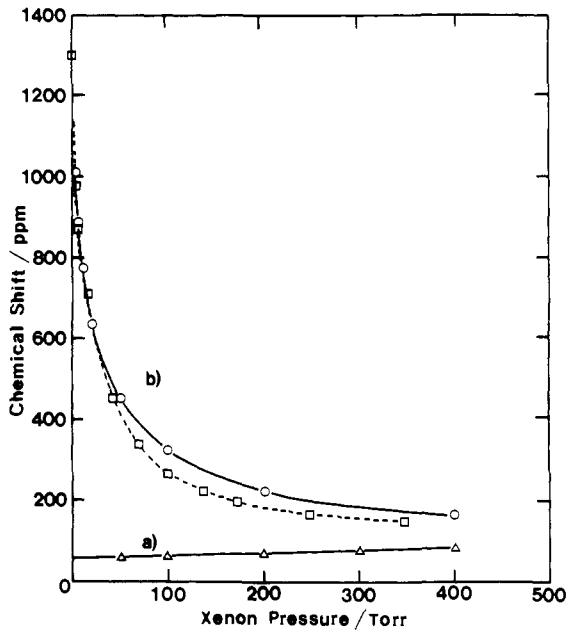

Figure 2. Chemical shift in the ^{129}Xe NMR spectrum of adsorbed xenon on NaY and $Pt_{7.1}/NaY$ plotted against pressure at 296 K: (a) NaY (△); (b) $Pt_{7.1}/NaY$, experimental (○) and calculated (□) with the assumption of rapid xenon exchange between Pt cluster and zeolite surfaces and δ_{Pt} = 1300 ppm.

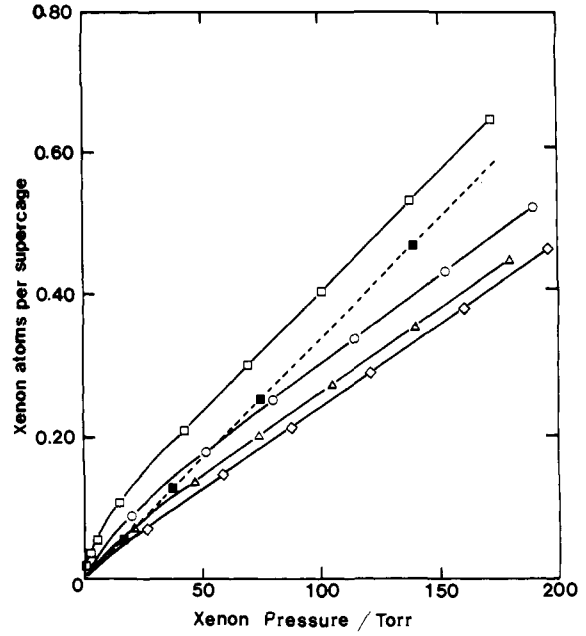

Figure 3. Xenon adsorption plotted against pressure: $Pt_{7.1}/NaY$ (○), $Pt_{3.6}/NaY$ (△), and $Pt_{1.4}/NaY$ (◇) at 310 K; $Pt_{7.1}/NaY$ (□) and $Pt_{7.1}/NaY$ with chemisorbed hydrogen (■) at 296 K. Xenon-adsorption isotherms from Pt/NaY samples at 296 and 310 K show a rapid increase in the adsorption at low pressure and then become linear with the pressure increase.

perature for 2 h. It was reduced further in flowing H_2 in the same way used for the preparation of Pt/NaY. The sample is designated as Ru_x/NaY. The xenon adsorption and the ^{129}Xe NMR experiment were performed at 296 K after the desorption of hydrogen at 673 K. The sample was also studied in situ after various treatments.

The ion exchange of $Pd(NH_3)_4^{2+}$ was carried out by stirring the zeolite powder in an aqueous ammonia solution of $PdCl_2$ overnight at room temperature. The O_2 activation and the reduction treatments were performed in the same way as for the Pt sample.

The xenon-adsorption isotherm was obtained by using a conventional volumetric gas-adsorption apparatus. The adsorption temperature was controlled to within ±0.1 K by a constant-temperature circulation bath since the xenon adsorption was very sensitive to the room temperature. For the ^{129}Xe NMR experiment, xenon gas was equilibrated with the sample at 296 K under given pressures. ^{129}Xe NMR spectra were obtained at 296 K with a Bruker AM 300 instrument operating at 83.0 MHz for ^{129}Xe with a 0.5-s relaxation delay. The chemical shift is referenced with respect to the NMR signal of the xenon in the bulk gas phase extrapolated to zero pressure.

A suspension of the fine sample powder (about 1 μm) in methanol was dropped onto microporous carbon grids and allowed to dry. Transmission electron micrographs of the thin edge of the zeolite crystal were taken with a JEM 2000-EX (JEOL) apparatus operating at 200 keV.

Results and Discussion

Figure 1 shows xenon-adsorption isotherms obtained from our high-purity NaY zeolite at various temperatures between 273 and 350 K. All the adsorption isotherms are nearly linear in the given pressure range, which indicates that the xenon adsorption on the zeolite fits for a very weak adsorption following Henry's law. Thus, the concentration of the adsorbed xenon increases almost proportional to the pressure under the present experimental conditions. The adsorbed xenon concentration can be related to the chemical shift in the ^{129}Xe NMR spectrum of xenon by $\delta = \delta_0 + \delta_1\rho + \delta_2\rho^2 + \ldots$, where δ_0 is a term taking into account various interactions between xenon and the zeolite surface, δ_1 and δ_2 are the proportionality constants, and ρ is the concentration of the adsorbed xenon.[3,10,15,23] The first-order term with respect to ρ is due to a binary xenon–xenon interaction, and the higher-order terms are due to higher-order interactions between xenon which are important only at very high ρ. Since ρ increases linearly with the pressure for the NaY zeolite, the ^{129}Xe NMR chemical shift also increases linearly with respect to the xenon pressure as Figure 2a shows, in good agreement with previous results.[3,15]

As Figure 3 shows, the xenon-adsorption isotherm obtained from the supported Pt sample is initially steep, progressively oblique, and then linear with the pressure increase above ca. 50 Torr. The degree of the initial steep increase is almost proportional to the Pt content, and the slope in the high-pressure linear part of the adsorption isotherm is the same for all samples containing 2.1 to 10.0% Pt (i.e., $Pt_{1.4}/NaY$ through $Pt_{7.1}/NaY$). Thus, as the Pt loading decreases to zero, the xenon-adsorption isotherm approaches a straight line which is parallel to the high-pressure linear part of the xenon-adsorption isotherm and passes through the origin. The heat of adsorption of xenon on the $Pt_{7.1}/NaY$ sample has been measured at 296 K by using the Clapeyron equation, $\Delta H_{ads}/R = [\partial \ln P/\partial(1/T)]_{N_s}$, for the xenon-adsorption isotherms obtained precisely at 293, 296, and 299 K, respectively. This ΔH_{ads} is plotted in Figure 4 as a function of the total amount of adsorbed xenon (N_s). An extrapolation of ΔH_{ads} to zero N_s corresponds to about 45 kJ mol^{-1}. However, the magnitude of ΔH_{ads} decreases with the increase of N_s, approaching an almost constant value of 23 kJ mol^{-1} above N_s equal to 0.15 Xe/supercage where the adsorption isotherms are nearly linear. This result suggests that the pressure-linear increase comes from the xenon adsorption on the zeolite support with ΔH_{ads} of about 20 kJ mol^{-1}, whereas the additional sharp increase appearing at low pressures comes from a strong xenon adsorption on the metal cluster surface with ΔH_{ads} of about 45 kJ mol^{-1}. After H_2 or O_2 was equilibrated to the $Pt_{7.1}/NaY$ samples at 1 atm for 30 min and subsequently evacuated at room temperature under 1×10^{-5} Torr, the sample gives a xenon-adsorption isotherm as if it has no Pt content, which indicates that the chemisorbed hydrogen on the Pt cluster surface hinders the strong adsorption of xenon.

It is possible to confirm the aforementioned strong adsorption of xenon on the Pt cluster from a quantitative analysis of ^{129}Xe NMR data of the adsorbed xenon gas. The amount of adsorbed xenon after hydrogen chemisorption corresponds to the xenon adsorption only on the zeolite support according to the above interpretation of the xenon-adsorption isotherm. The difference of the adsorption isotherms obtained respectively before and after the hydrogen or oxygen chemisorption equals the amount of xenon adsorbed strongly on the metal cluster surface, which is nearly saturated above 50 Torr. With the assumption that xenon can

(23) Suh, D. J.; Park, T.-J.; Ihm, S.-K.; Ryoo, R. *J. Phys. Chem.* **1991**, *95*, 3767.

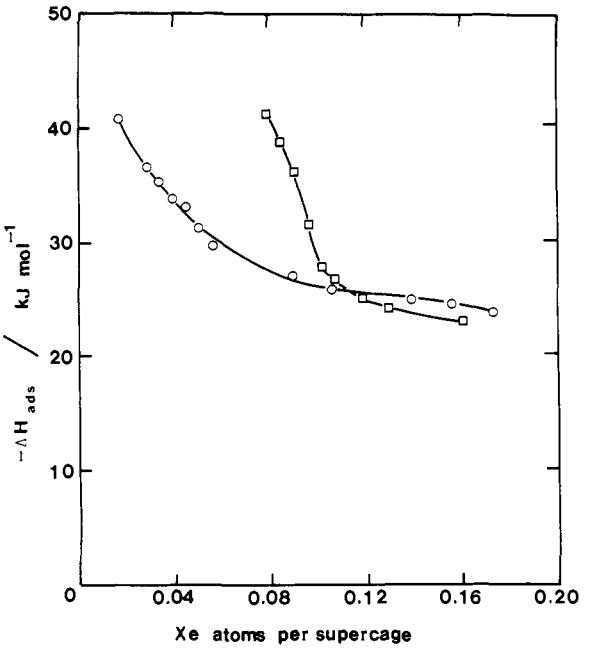

Figure 4. Heats of adsorption of xenon on $Pt_{7.1}$/NaY (○) and $Ru_{6.2}$/NaY (□) plotted as a function of the total amount of adsorbed xenon (i.e. N_s).

Table II. Numerical Data Used for the Calculation of Chemical Shift of Adsorbed Xenon on $Pt_{7.1}$/NaY and the Results of the Calculation

pressure, Torr	n_{ads}[a]	n_{Pt}[a]	n_{sup}[a]	δ_{NaY}[b]	δ_{cal}[c]
2.8	2.12	1.57	0.55	60.2	979.2
5.6	3.22	2.12	1.10	60.3	875.4
15.3	6.28	3.29	2.99	60.9	710.7
42.7	12.21	3.86	8.35	62.7	453.8
69.3	17.45	3.90	13.54	64.3	340.8
100.0	23.33	3.79	19.54	66.2	266.4
137.3	30.70	3.87	26.83	68.6	223.9
171.5	37.38	3.87	33.51	70.7	197.8
246.4	52.13	3.98	48.16	75.4	168.8
346.3	71.73	4.01	67.66	81.6	150.7

[a] Units of 10^{-5} mol g^{-1}. n_{ads} and n_{sup} are from the xenon-adsorption isotherms determined before and after hydrogen chemisorption at 296 K shown in Figure 3, respectively. [b] δ_{NaY} is the experimental value for the chemical shift of xenon on NaY under a given pressure. [c] δ_{cal} is calculated from eq 1 with δ_{Pt} = 1300 ppm.

exchange very rapidly between the metal cluster and the zeolite support,[14,19] the chemical shift in the ^{129}Xe NMR spectrum of the adsorbed xenon gas can be written as

$$\delta = \{n_{Pt}\delta_{Pt} + n_{sup}\delta_{sup}\}/(n_{Pt} + n_{sup}) \quad (1)$$

where n_{Pt} and δ_{Pt} are the amount and the chemical shift of xenon adsorbed on the cluster, and n_{sup} and δ_{sup} are those on the support, respectively. δ_{sup} is approximately the same as the chemical shift of xenon adsorbed on the NaY zeolite under the same pressure. With a value of δ_{Pt} = 1300 ppm, a good fit has been obtained for the experimental values, as shown in Figure 2b. Values of n_{Pt}, n_{sup}, and δ_{sup} used for the calculation of δ are listed in Table II. The assumption of a rapid exchange in ^{129}Xe NMR studies can be good at low xenon pressures,[24] and therefore the best fit at low pressures has been made. The discrepancy at higher pressures seems to come mainly from a decrease in the xenon exchange efficiency due to a diffusional hindrance by highly concentrated xenon. But such a small discrepancy between the experimental and theoretical data is not significant in describing the nature of the xenon exchange. Although we have started to make such an analysis of the chemical shift simply in order to confirm the nature

(24) Cheung, T. T. P. *J. Phys. Chem.* **1989**, *93*, 7549.

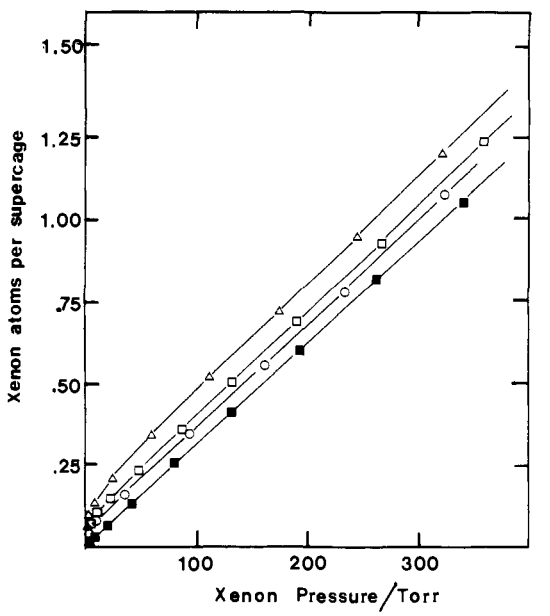

Figure 5. Xenon adsorption plotted against pressure: (△) $Ru_{9.3}$/NaY; (□) $Ru_{6.2}$/NaY; (○) $Ru_{3.1}$/NaY; (■) $Ru_{9.3}$/NaY with chemisorbed hydrogen. Xenon-adsorption isotherms obtained from Ru/NaY samples at 296 K are similar to those from Pt/NaY in Figure 3.

of strong interaction between xenon and the supported cluster, it is also possible to find that δ_{Pt} thus obtained is the chemical shift of xenon adsorbed on the Pt cluster surface. We have determined δ_{metal} for other group VIII metal clusters supported on Y zeolite in the same way as described for the Pt sample. The magnitude of δ_{metal} for the zeolite-supported metal clusters ranges widely from ca. 500 to 3500 ppm, indicating that it can be influenced by the type and size of the metal: 800 ± 50 ppm for a bimetallic PtCu cluster,[25] 800 ± 50 for Ir, 1300 ± 50 for Pt, 950 ± 50 for a Ru sample with the cluster size of 1 nm, 550 ± 50 for a Ru sample of less than 1 nm, 3000 ± 200 for Pd,[26] and 3200 ± 400 for Rh. Ahn et al. reported that a decrease of δ_{metal} from 1300 to 800 ppm was due to the formation of a bimetallic cluster following reduction of Cu^{2+} to Cu^0 on Pt clusters in the zeolite supercage.[25] Thus, δ_{metal} may be used as a suitable parameter for the study of monometallic and bimetallic clusters supported on zeolite.

Figure 5 shows xenon adsorption isotherms obtained from several Ru/NaY samples which have been prepared by evacuating the Ru precursors at 673 K, reducing in H_2 at 673 K, and then desorbing the dihydrogen at the same temperature. All the isotherms indicate a strong adsorption of xenon on the Ru cluster and a weak adsorption on the zeolite support, very similar to the above results obtained from the Pt/NaY samples. The heat of adsorption of xenon on $Ru_{6.2}$/NaY sample is larger than that on $Pt_{7.1}$/NaY at low pressure as Figure 4 shows. The chemical shift in the ^{129}Xe NMR spectrum of the adsorbed xenon gas can also be fit by a rapid xenon exchange between the metal cluster and the zeolite support in the same way as for the Pt/NaY sample. Here the best-fitting δ_{Ru} in Figure 6 is 950 ppm, which is smaller than δ_{Pt} by 350 ppm. The amount of xenon adsorption for the saturation on the Pt or Ru cluster can be determined from an intercept of a line extrapolating the linear part of the adsorption isotherm to zero pressure in the case where a similar extrapolation of a xenon-adsorption isotherm obtained after the chemisorption of hydrogen (or oxygen) gives a negligible value. The high-purity NaY zeolite samples used in this work indeed give a practically zero intercept as listed in Table III. Our results show that the saturation quantity, obtained by such an extrapolation of the adsorption isotherm, has been found to remain practically constant

(25) Ahn, D. H.; Lee, J. S.; Nomura, M.; Sachtler, W. M. H.; Moretti, G.; Woo, S. I.; Ryoo, R. *J. Catal.* In press.
(26) Kim, J.-G.; Ihm, S.-K.; Lee, J. Y.; Ryoo, R. *J. Phys. Chem.* In press.

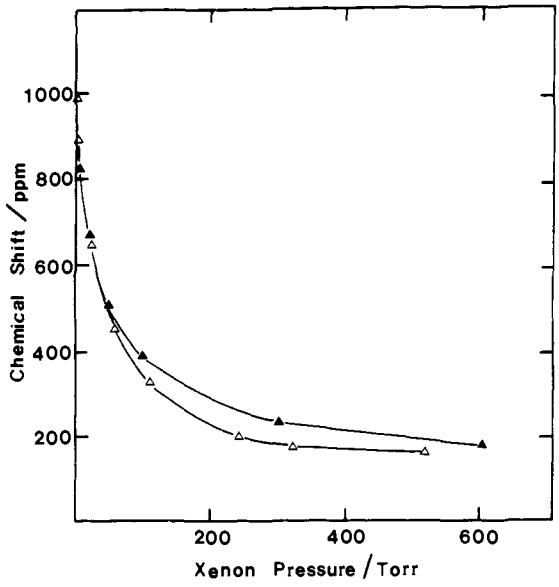

Figure 6. Chemical shift plotted against xenon pressure: (▲) experimental; (△) calculated with the assumption of a rapid xenon exchange between Ru cluster and zeolite surfaces and δ_{Ru} = 950 ppm. Chemical shift in the ^{129}Xe NMR spectrum of adsorbed xenon on $Ru_{9.3}/NaY$ decreases with the pressure increase, similar to that from Pt/NaY.

Table III. Average Number of Metal Atoms per Cluster (N) from the Xenon-Adsorption Method Proposed in This Work

sample	n_{metal} satd[a]	N	δ,[b] ppm
NaY			84
$Pt_{7.1}/NaY$	6.3×10^{-2}	56	169
$Pt_{3.6}/NaY$	3.1×10^{-2}	58	128
$Pt_{1.4}/NaY$	1.2×10^{-2}	61	101
$Ru_{9.3}/NaY$[c]	1.4×10^{-1}	32	213
$Ru_{6.2}/NaY$[d]	7.7×10^{-2}	40	142
$Ru_{6.2}/NaY$[c]	5.5×10^{-2}	56	144
$Ru_{3.1}/NaY$[c]	3.1×10^{-2}	49	115
$Ru_{6.2}/NaY$[e]	1.6×10^{-3}		84
$Pd_{6.6}/CaY$	5.0×10^{-2}	67	393
$Pd_{7.1}/YX$	4.5×10^{-2}	78	400

[a] Extrapolating n_{metal} in the range of 50–300 Torr at 296 K to zero pressure, in terms of xenon atoms per supercage. [b] Chemical shift in the ^{129}Xe NMR spectrum of adsorbed xenon under 400 Torr at 296 K. [c] The precursor was heated under vacuum to 673 K over 6 h and then for 2 h in H_2 at 673 K. [d] Same as footnote *c* except for increasing temperature to 673 K over 50 h. [e] This sample was treated in O_2 at 673 K and then reduced in H_2 at 673 K.

over the adsorption temperature range between 273 and 350 K although the pressure at which xenon becomes saturated on the metal cluster increases with the adsorption temperature. Figures 7 and 8 illustrate that the determination of the amount of xenon adsorption for the saturation on the Ru clusters after various treatments can probe the cluster size variation with great ease and high precision. A rapid increase in the xenon quantity coming after the vacuum treatment above 573 K indicates that the Ru cluster begins to form by an autoreduction during the vacuum treatment of the precursor above 573 K.[27] A gradual decrease of the xenon quantity as a function of the heating temperature above 623 K can be explained if the Ru cluster grows because of the heat treatment. Our transmission electron micrographs[27] show only small clusters of about 1 nm even after prolonged heating at 673 K. There is no indication by TEM and ^{129}Xe NMR spectroscopy for the Ru cluster agglomeration onto the external surface of zeolite after this heat treatment in vacuum or H_2.[27] It therefore appears that the Ru clusters grow in a supercage or agglomerate over a few adjacent supercages with the heat treatment. Figure 8 indicates that the cluster can grow very large upon treatment in O_2 even at much lower temperatures, e.g. 423

(27) Ryoo, R.; Cho, S. J.; Jung, S.; Shul, Y. G.; Lee, J. Y., in preparation.

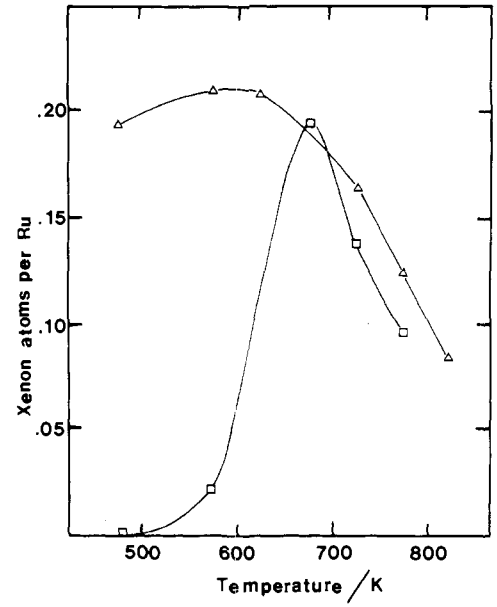

Figure 7. The total amount of xenon adsorbed on the Ru cluster under saturation plotted against the sample treatment temperature: (□) evacuation of a precursor of $Ru_{9.3}/NaY$ sample showing a rapid increase at 573 K due to clustering; (△) further reduction of this sample by H_2 after evacuation at 673 K showing a decrease above 673 K due to the cluster growth.

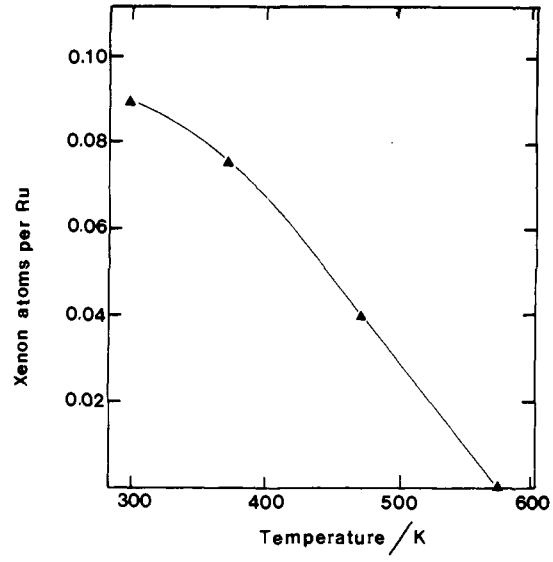

Figure 8. Xenon adsorption on Ru plotted against the sample treatment temperature. The total amount of xenon adsorbed on the Ru cluster under saturation decreases after treatment in O_2 at a given temperature and a subsequent reduction at 673 K, in agreement with the formation of a large agglomeration of Ru species during the treatment in O_2.

K, probably because RuO_2 formed by the oxidation treatment is highly volatile, migrates onto the external surface of the zeolite, and maintains its size during a subsequent reduction treatment. Such a migration of Ru species through the formation of RuO_2 agrees with previous results obtained by Verdonck et al.[28] and Pederson and Lunsford[22] but disagrees with those of Shoemaker and Apple.[13] In fact, large Ru agglomerations can clearly be seen in our transmission electron micrograph in Figure 9 after the O_2-treated cluster is reduced by H_2.

Commercial NaY zeolite samples often show a significantly different value from the extrapolation of the xenon-adsorption isotherm, which can probably come from strong xenon adsorption on the impurities or the structural defects in the zeolite. YX and

(28) Verdonck, J. J.; Jacobs, P. A.; Genet, M.; Poncelet, G. *J. Chem. Soc., Faraday Trans. 1* **1980**, *76*, 403.

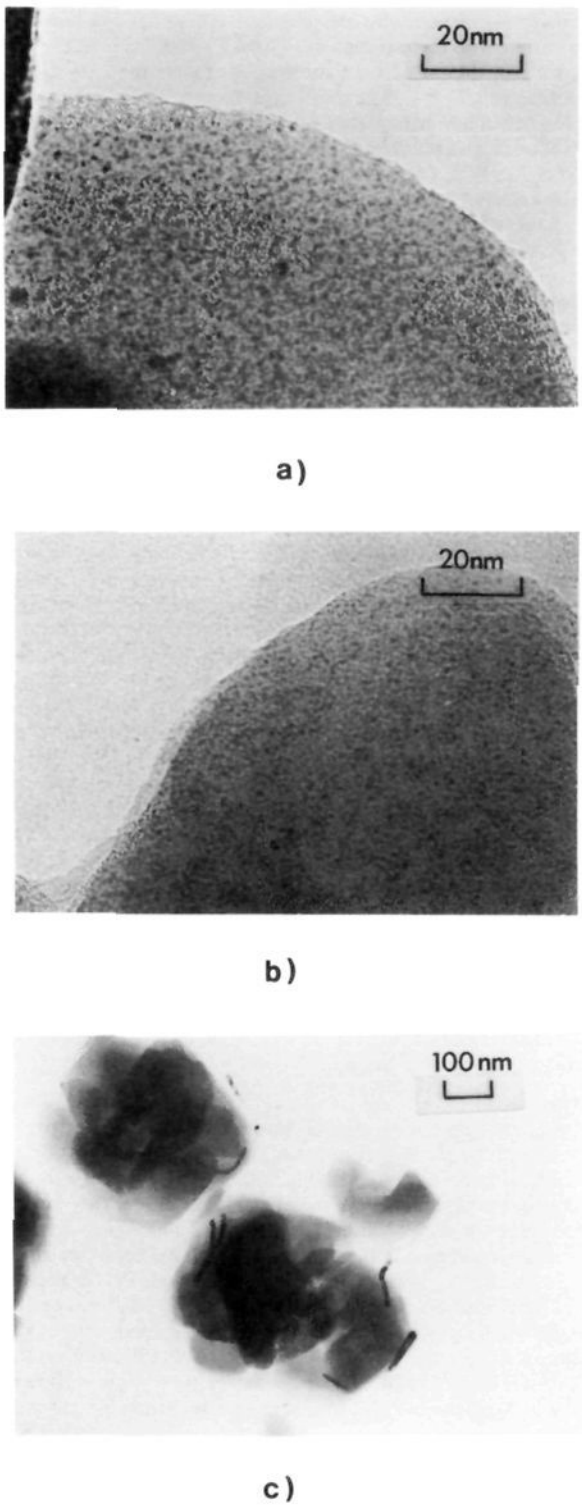

Figure 9. Transmission electron micrographs from (a) $Pt_{7.1}/NaY$ and (b) fresh $Ru_{6.2}/NaY$ sample exposed to air at room temperature and (c) after heating in O_2 at 673 K and subsequent reducing at 673 K.

CaY zeolite samples also give a xenon-adsorption isotherm with a significant curvature due to xenon adsorption on the multivalent cation.[26] For such a zeolite support which gives a curved xenon-adsorption isotherm, the saturation quantity of xenon on the metal clusters is difficult to obtain from a direct extrapolation of a xenon-adsorption isotherm (see Figure 10). Instead, the quantity has been determined by extrapolating the difference between the xenon-adsorption isotherms obtained respectively before and after the hydrogen chemisorption in a sufficiently high

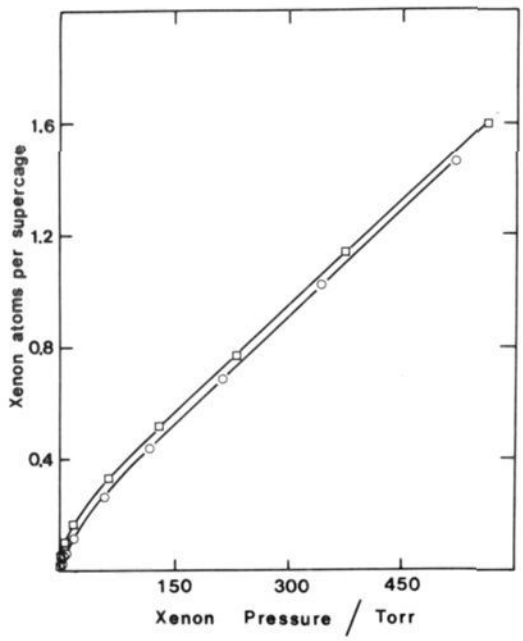

Figure 10. Xenon adsorption plotted against pressure: fresh sample (□) and sample with chemisorbed hydrogen (○). The difference of the xenon adsorption isotherms for $Pd_{7.1}/YX$ sample at 296 K is due to the inhibition of strong xenon adsorption on the Pd cluster by chemisorbed hydrogen.

Table IV. ^{129}Xe NMR Chemical Shift,[c] Saturation Quantity for Xenon Adsorption on Pd, and Pd Cluster Size Obtained by TEM[26]

sample	$\Delta\delta$,[a] ppm	n_{Pd} satd[b]	size by TEM, nm
$Pd_{7.0}/NaY$	151	2.1	2
$Pd_{5.8}/YY$	115	2.0	2
$Pd_{6.6}/CaY$	273	5.0	1
$Pd_{7.0}/NaX$	168	2.4	2
$Pd_{7.1}/YX$	298	4.5	1

[a] $\Delta\delta = \delta_{sample} - \delta_{sample\ satd\ by\ H\ at\ 296\ K}$. [b] In terms of xenon atoms per supercage × 10^{-2}. [c] A decrease in the ^{129}Xe NMR chemical shift occurred with hydrogen chemisorption under 400 Torr of xenon.

pressure region, e.g. above 50 Torr to zero pressure. Table IV lists the xenon-saturation quantity obtained from various Pd/Y and Pd/X samples in this manner. Since the amount of xenon adsorbed on the metal clusters and the chemical shift of xenon increase with decreasing cluster size (or increasing total Pd surface area), all the data including those from TEM indicate that the use of YX and CaY zeolite supports can give much smaller Pd clusters, compared with other zeolites. It appears that the cluster size is closely related to the xenon-adsorption ability of zeolite support. The curvature in the xenon-adsorption isotherm suggests that YX and CaY zeolites have relatively strong xenon-adsorption ability. All the other zeolite supports in Table IV, including YY, give a linear type of xenon-adsorption isotherms. Therefore, the multivalent cations in the zeolite wall, which can attract xenon, are also considered to adsorb Pd species formed during the reduction, thus inhibiting the migration of Pd cluster into large agglomerations. In this way, the xenon-adsorption method proposed here can easily clearlify an earlier suggestion that small Pd clusters can be formed in the zeolite supercage by a chemical anchoring mechanism due to multivalent cations.[26,29] Details of this work on the supported Pd cluster were reported recently.[26] Rh and Ir clusters supported on NaY zeolite also have considerably strong interaction with xenon, similar to other metal clusters discussed above.

The xenon adsorption technique suggested in this paper has been shown above to be very useful in probing the metal cluster for-

(29) Homeyer, S. T.; Sheu, L. L.; Zhang, Z.; Sachtler, W. M. H.; Balse, V. R.; Dumesic, J. A. *Appl. Catal.* **1990**, *64*, 225.

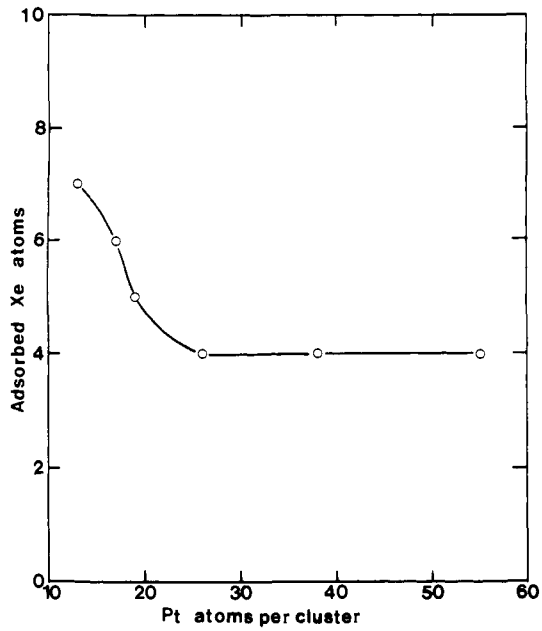

Figure 11. Plot of the maximum number of xenon atoms in direct contact with a Pt cluster in zeolite supercage obtained by using space-filling chemical models of xenon and Pt cluster in the supercage as a function of the number of Pt atoms per cluster.

mation and growth in zeolites in a comparative manner. It will be further exciting if the absolute information on the cluster size such as the average number of metal atoms per cluster can be determined from the xenon-adsorption data. A few assumptions are taken here for this purpose as described below. The number of xenon atoms saturated on a metal cluster will depend on the size and geometry of the cluster. Here we may assume a nearly spherical geometry for our Pt cluster supported on NaY zeolite, since previous studies using TEM, EXAFS, and WAXS agreed with bulk-like face centered cubic structure with a fairly large average coordination number (e.g. 7.0 or 8.8)[5] for small Pt clusters which were supported on Y zeolites practically in the same way used in the present work. Molecular models of xenon and metal cluster in zeolite supercage can then be used to assume the number of saturated xenon atoms to be the maximum number of xenon atoms (Z) that can be in contact with the surface of the metal cluster. For Pt clusters consisting of 26–55 atoms in the supercage, Z may be assumed to be 4 because only one 0.43-nm xenon atom can be in direct contact with the cluster in this size range through a supercage aperture of 0.74-nm diameter. For a Pt cluster smaller than this size range, xenon will be able to enter the supercage containing the cluster, and therefore Z will be greater than 4. The number Z in such a case can depend to a certain degree on the location of the cluster within the supercage. We have assumed that the cluster is most likely to contact one or more six-membered oxygen rings in the supercage. The Z values thus obtained are plotted as a function of the number of Pt atoms per cluster in Figure 11. With these results and assumptions, the average number of metal atoms per cluster (N) can be obtained as $N = ZM/G$, where M is the total number of metal atoms in the sample and G is an experimental value for the total number of xenon atoms corresponding to the strong adsorption on the metal clusters in the sample. The value of N thus obtained can verify the assumption used for Z. Using successive iteration with a new value of Z until N and Z are in agreement, the value of N can be obtained in a self-consistent manner. For example, we have obtained 3.6 ($\pm$0.2) $\times 10^{-5}$ mol of xenon per gram of $Pt_{7.1}/NaY$ sample from the difference in xenon adsorption isotherms occurring with hydrogen chemisorption, which corresponds to 6.3 ($\pm$0.3) $\times 10^{-2}$ Xe/supercage for G as listed in Table III. M for $Pt_{7.1}/NaY$ is 7.1 Pt atoms per unit cell of zeolite (0.89 Pt atom per supercage). Starting with the assumption that the average number of Pt atoms per cluster is close to 13, we get 7 Xe/cluster for Z from Figure 11. Thus, we obtain $N = ZM/G = (7 \times 0.89)/(6.3 \times 10^{-2})$ Pt/cluster = 99 Pt atoms per cluster. This result is however incompatible with the assumption of 7 for Z. Using a new Z value of 4, we can then obtain 56 atoms per cluster for N which is compatible with $Z = 4$. The result summarized in Table III agrees with the size of approximately 1 nm obtained from our TEM data, as well as similar sizes determined previously by others using TEM, EXAFS, WAXS, and SAXS for the supported Pt samples prepared similarly.[4-9] A Pt cluster consisting of about 50 atoms will be as large as necessary to fit into a supercage of 1.3 nm.

In Table III, the chemical shift in the ^{129}Xe NMR spectrum of adsorbed xenon gas on various samples has been compared with the average number of metal atoms per cluster determined by the present xenon-adsorption method. The magnitude of the chemical shift for our Pt samples agrees with previous results.[3,5] However, our Ru samples give several times higher chemical shifts (with respect to NaY) than previous data[13] under the identical conditions extrapolated to the same metal loadings, which is probably due to better metal dispersion or different metal location in our case using ammine complexes. No other previous studies on zeolite-supported Pd cluster by ^{129}Xe NMR spectroscopy are known to us. Details of our ^{129}Xe NMR data for Pd are reported elsewhere.[26] Thus, the chemical shift in ^{129}Xe NMR data is very useful for the detection of various chemical changes in the zeolite sample. However, its value may not be compared directly between samples of different metals since the chemical shift depends on the nature of the metal cluster as well as its dispersion. The size of the metal cluster is very difficult to determine by ^{129}Xe NMR studies. On the contrary, the xenon-adsorption method proposed here has particularly high precision to give the information on the size of metal clusters supported on Y zeolite, independent of the metal if the metal cluster has a strong interaction with xenon. Its accuracy for the determination of the average number of metal atoms per cluster depends greatly on the assumptions made in this work. In the case where the cluster size distribution is very wide or the cluster exceeds the size of the supercage, the total amount of xenon adsorption on metal clusters determined by this method may be enough to compare the cluster size variation even if it fails to give the average number of metal atoms per cluster with reasonable accuracy. This has been demonstrated in a previous study which indicates that there exists an anchoring effect due to multivalent cations on the formation of Pd clusters in the supercage of X and Y zeolites.[26]

Conclusion

The xenon-adsorption method proposed in the present paper has been shown to be very precise and useful for the study of cluster formation and growth on zeolite. The approach to determine the average number of metal atoms per cluster can provide a good value for the Pt/NaY samples with a sufficiently narrow cluster size distribution in the supercage, which has been confirmed by TEM and ^{129}Xe NMR data obtained from our Pt/NaY samples. The Pt clusters seems to contain about 50–60 atoms on the average, which may be filled in a supercage, independent of the Pt content between 2 and 10%. For other metal samples, the assumption of spherical cluster geometry may need sufficient evidence. But it can be concluded, from a comparison of the xenon saturation quantities between different metal samples, that Ru clusters can be prepared in a much smaller size than the Pt cluster in the supercage. The advantage of the present method in studying the metal clusters supported on Y or X zeolite is that it uses the physisorption of xenon on the metal cluster, and therefore the method is independent of metal only if xenon can be adsorbed significantly more strongly on the metal cluster than on the zeolite surface.

Acknowledgment. R. Ryoo is grateful to Prof. M. Boudart for helpful discussions on the Pt cluster supported on Y zeolites. This work was financially supported by Korea Science and Engineering Foundation.

Registry No. ^{129}Xe, 13965-99-6; Xe, 7440-63-3; $[Pd(NH_3)_4]Cl_2$, 13815-17-3; $[Pt(NH_3)_4]Cl$, 13933-32-9; $Ru(OH)_3$, 12135-42-1; H_2, 1333-74-0; O_2, 7782-44-7; K, 7440-09-7; Ca, 7440-70-2; Y, 7440-65-5; Pt, 7440-06-4; Ru, 7440-18-8; Pd, 7440-05-3.